

# Anandamide extends platelets survival through CB<sub>1</sub>-dependent Akt signaling

Maria Valeria Catani · Valeria Gasperi ·  
Daniela Evangelista · Alessandro Finazzi Agrò ·  
Luciana Avigliano · Mauro Maccarrone

Received: 19 June 2009 / Revised: 12 October 2009 / Accepted: 30 October 2009 / Published online: 20 November 2009  
© Birkhäuser Verlag, Basel/Switzerland 2009

**Abstract** Platelets are stored at 22°C, since incubation at 37°C results in loss of viability. Nonetheless, in our body (37°C), platelets survive for 8–10 days. This discrepancy has been explained in terms of deprivation of viability factors or accumulation of apoptotic factors during storage. We report that the endocannabinoid anandamide (AEA) may be one of the agents allowing platelet survival. In fact, at 37°C, human platelets enhance the expression of proapoptotic proteins (caspases, Bax, Bak) and decrease the expression of Bcl-xL, thus changing the Bcl-xL/Bak ratio, a key platelet biological clock. AEA or its non-hydrolyzable analogue, methanandamide, extend platelet life span, without reversing the changes in Bcl-xL/Bak ratio induced by heat stress. Instead, AEA binding to type-1 cannabinoid receptor activates Akt, which regulates, through phosphorylation of Bad, the interactions among different Bcl-2

family members. These findings could have implications for platelet collection and, potentially, for their clinical use.

**Keywords** Bcl-xL · Bak · Cell death · Endocannabinoid system · Signal transduction · Thrombocytopenia

## Introduction

*N*-Arachidonylethanolamine (anandamide, AEA) is a lipid molecule belonging to the family of endocannabinoids (eCBs) [1, 2]. AEA is synthesized “on demand” from membrane precursors by a specific *N*-acyl-phosphatidyl-ethanolamine hydrolyzing phospholipase D and, once released, it binds to type-1 or type-2 cannabinoid (CB<sub>1</sub> and CB<sub>2</sub>) receptors, and to other non-CB targets, such as type-1 vanilloid receptor (transient receptor potential vanilloid type 1, TRPV1) [1, 2]. The biological activity of AEA at its receptors is terminated by selective uptake through a purported AEA membrane transporter [3], followed by intracellular hydrolysis catalyzed by the fatty acid amide hydrolase (FAAH) [4]. eCBs, together with the proteins that bind and metabolize them, form the so-called “endocannabinoid system” [1, 2].

To date, an ever-growing body of evidence supports a key role for the endocannabinoid system in the pathophysiology of the central nervous system [5] and peripheral tissues [6]. A general effect of eCBs is to control cell survival and death, by acting as pro- or anti-apoptotic agents depending on the cell type and the receptor engaged [7, 8]. eCBs induce cell death in a variety of experimental models, including neurons [9], erythrocytes [10], hepatocytes [11], sebocytes [12], and blastocysts [13]. On the other hand, (endo)cannabinoids are able to modulate,

---

M. V. Catani and V. Gasperi are equally first authors; L. Avigliano and M. Maccarrone are equally senior authors.

---

**Electronic supplementary material** The online version of this article (doi:10.1007/s00018-009-0198-9) contains supplementary material, which is available to authorized users.

---

M. V. Catani · V. Gasperi · D. Evangelista ·  
A. Finazzi Agrò · L. Avigliano  
Department of Experimental Medicine and Biochemical  
Sciences, University of Rome Tor Vergata, Via Montpellier 1,  
00133 Rome, Italy

V. Gasperi · M. Maccarrone  
European Center for Brain Research (CERC)/IRCCS S. Lucia  
Foundation, Via Ardeatina 306, 00179 Rome, Italy

M. Maccarrone (✉)  
Department of Biomedical Sciences, University of Teramo,  
Piazza A. Moro 45, 64100 Teramo, Italy  
e-mail: mmaccarrone@unite.it

through CB<sub>1</sub> receptors, the phosphatidylinositol 3-kinase/protein kinase B (PI3K/Akt) pathway, which serves as a pivotal anti-apoptotic signal [14, 15].

eCBs also play a critical role in the vascular system, where they are released from endothelial cells, lymphocytes, macrophages, and platelets (PLTs). In particular, it has been clearly demonstrated that eCBs may promote PLTs activation, alone or synergistically with classical platelet agonists [16–19], supporting a potential role as thrombogenic and atherosclerotic agents [17]. Consistently, PLTs are able to metabolize circulating eCBs, thus regulating their endogenous tone in the periphery [18, 19].

PLTs are small, anucleated cytoplasmic fragments derived from megakaryocytes, which are formed in bone marrow, lungs, and blood [20]. Human megakaryocytes release PLTs into the blood stream, where they circulate for about 10 days; afterwards, PLTs are destroyed in liver and spleen. Several mechanisms regulating platelet biogenesis have been disclosed in recent years [21, 22]. Yet, very little is known about the mechanism(s) accounting for their survival, once they are released from megakaryocytes. It has been shown that PLT survival both in vivo and in vitro depends strictly on time and temperature, although it is still unclear how PLTs sense the heat challenge. Indeed, PLTs for transfusion are usually stored at 22°C for no longer than 5 days, since storage at 37°C dramatically accelerates cell death, that already becomes evident after 24–48 h [23]. More recently, some factors controlling PLT survival have been identified. Like nucleated cells, PLTs are intrinsically programmed to die, as they contain the complete apoptotic machinery. PLTs express both Bcl-xL and Bak, two proteins of the Bcl-2 family that show antagonizing effects, and that seem to represent a molecular clock responsible for platelet life span [24]. It should be noted that cell survival is promoted by Bcl-xL [25], whereas Bax or Bak are required for commitment to death [26]. When activated, Bax or Bak can permeabilize the outer membrane of mitochondria, thus allowing cytochrome *c* release and downstream activation of caspases, which in turn dismantle the cell [25, 26]. Against this background, we sought here to investigate whether eCBs may modulate the life/death balance of PLTs, thus implying an involvement of these lipid mediators in the clearance of platelets from the circulation.

## Materials and methods

### Reagents

Chemicals were of the purest analytical grade. AEA, arachidonic acid (AA), 1-(2,4-dichlorophenyl)-5-(4-iodophenyl)-4-methyl-*N*-4-morpholinyl-1H-pyrazole-3-carboxamide

(AM281) and 3-[4,5-diethylthiazol-2-yl]-2,5-diphenyltetrazolium bromide (MTT) were purchased from Sigma Chemical (St. Louis, MO, USA). Iodo-resiniferatoxin (IRTX) and (6aR,10aR)-3-(1,1-dimethylbutyl)-6a,7,10,10a-tetrahydro-6,6,9-trimethyl-6H-dibenzo[*b,d*]pyran (JWH133) were from Tocris (Bristol, UK). *N*-Piperidino-5-(4-chlorophenyl)-1-(2,4-dichlorophenyl)-4-methyl-3-pyrazolecarboxamide (SR141716) and *N*-[1(*S*)-endo-1,3,3-trimethylbicyclo[2.2.1]-heptan-2-yl]-5-(4-chloro-3-methyl phenyl)-1-(4-methylbenzyl) pyrazole-3-carboxamide (SR144528) were kind gifts of Sanofi-Aventis Recherche (Montpellier, France). Methanandamide (Met-AEA), (*S*)-1'-(4-hydroxybenzyl)-oleoylethanolamide (OMDM1), cyclohexyl carbamic acid 3'-carbamoyl-biphenyl-3-yl ester (URB597), wortmannin and arachidonyl-2-chloroethylamide (ACEA) were from Alexis (Lausen, Switzerland). Rabbit antibodies against Bad, Bak, Bcl-xL or Bax, and mouse antibody raised against protein kinase B (Akt) were from Cell Signalling Technology (Danvers, MA, USA). Rabbit anti-phospho-Bad<sup>Ser134</sup> antibodies were from Abnova (Buckingham, UK). Goat antibodies against actin, mouse antibodies against caspase 9 and Bcl-xL, rabbit antibodies against phospho-Akt<sup>Ser473</sup>, as well as secondary antibodies conjugated to horseradish peroxidase and enhanced chemiluminescence (ECL) kit were from Santa Cruz Biotechnology (Santa Cruz, CA, USA). Secondary antibodies conjugated to alkaline phosphatase and nonfat dry milk were from Bio-Rad (Hercules, CA, USA).

### Isolation of platelets

After informed consent, blood samples were collected from healthy subjects (age range 20–40 years), using ACD (112 mM glucose, 130 mM citric acid, 152 mM sodium citrate) as anticoagulant. Whole blood was centrifuged at 150g for 10 min, and platelet-rich plasma (PRP) was centrifuged again in order to remove all contaminant red and white blood cells. PLTs were pelleted from PRP by centrifugation at 1,000g for 15 min, and were resuspended in Tyrode's buffer (100 mM Hepes, 1.3 M NaCl, 29 mM KCl, 120 mM NaHCO<sub>3</sub>, pH 7.4), containing 1/10 (v/v) ACD and 2 mM glucose. Platelet concentration was adjusted to 3 × 10<sup>8</sup> cells/mL with Tyrode's buffer.

### Platelet viability

Cell viability was evaluated by measuring the mitochondrial reduction of MTT to formazan, according to the manufacturer's protocol. Briefly, PLTs were centrifuged at 1,000g for 15 min and resuspended in 500 μl of dye solution (0.5 mg/ml MTT in Tyrode's buffer). After incubation at 37°C for 2 h, PLTs were centrifuged again and

the insoluble formazan dye was dissolved with 100  $\mu$ l DMSO before reading the absorbance at 590 nm.

### Immunoprecipitation

Immunoprecipitation was performed with the Protein G Immuprecipitation Kit (Sigma–Aldrich), according to the manufacturer's instructions. Briefly, PLTs were lysed in CHAPS buffer (20 mM HEPES pH 7.4, 10 mM KCl, 1.5 mM MgCl<sub>2</sub>, 1 mM EDTA, 0.25 M sucrose, 2% CHAPS), containing a protease inhibitors cocktail (Sigma–Aldrich) and phosphatase inhibitors (20 mM  $\beta$ -glycerophosphate, 10 mM NaF, 1 mM Na<sub>3</sub>VO<sub>4</sub>). Then, they were centrifuged at 15,000g for 20 min at 4°C. Supernatant proteins (300  $\mu$ g) were precleared with 30  $\mu$ l of a 1:1 slurry of protein G-agarose in immunoprecipitation buffer for 3 h at 4°C, and were incubated with mouse anti-Bcl-xL antibodies (2  $\mu$ g) overnight at 4°C. Immunocomplexes were then precipitated with protein G-agarose for 3 h at 4°C. After washings, bound proteins were eluted with 60  $\mu$ l of SDS–PAGE sample buffer, boiled at 95°C for 5 min and an aliquot (20  $\mu$ l) was analyzed by western blotting.

### Western Blotting

PLTs were lysed in RIPA buffer (phosphate buffered saline (PBS), 1% Nonidet P40, 0.5% sodium deoxycholate, 0.1% SDS), containing protease and phosphatase inhibitors. Cell lysates were subjected to SDS–PAGE, electroblotted onto PVDF membranes, incubated with specific antibodies and detected with ECL. The specific primary antibodies used were: anti-Bad (1:500), anti-phospho-Bad (1:500), anti-Bak (1:500), anti-Bax (1:500), anti-Bcl-xL (1:500), anti-caspase 9 (1:100), anti-Akt (1:1,000) anti-phospho-Akt (1:200).

To analyze Bak and Bax oligomerization, total proteins were run under non-reducing conditions and were incubated with the corresponding antibodies.

### Caspase 3 activity

Caspase 3 Colorimetric Assay Kit (Biovision, CA, USA) was used to assess caspase 3 activity in PLTs. Briefly, platelet cytosolic extracts (25  $\mu$ g of proteins) were incubated with 200  $\mu$ M DEVD-*p*-nitroaniline (DEVD-*p*NA) fluorogenic substrate at 37°C for 2 h, and absorbance was read at 405 nm.

### Cell subfractionation and enzyme-linked immunosorbent assay

PLTs were lysed in HB buffer (5 mM Tris–HCl pH 7.4, 10 mM KCl, 1 mM MgCl<sub>2</sub>, 1 mM DTT), containing

protease inhibitor cocktail, and were centrifuged at 1,000g for 10 min to completely remove nuclei and whole cells. The resulting supernatant was centrifuged at 3,000g for 10 min; the pellet was saved as membrane-bound organellar fraction enriched with mitochondria, while the supernatant, after centrifugation at 100,000g for 40 min, was collected as cytosolic fraction. These two fractions were analyzed for cytochrome *c* localization by means of enzyme-linked immunosorbent assay (ELISA), as reported [27]. Briefly, mitochondrial and cytosolic proteins (20  $\mu$ g/well) were incubated with anti-cytochrome *c* antibody (diluted 1:500), and then with an alkaline phosphatase-conjugated secondary antibody.

### Statistical analysis

Data reported are the mean  $\pm$  SD of at least three independent experiments, each performed in duplicate. Statistical analysis was performed by the nonparametric Mann–Whitney *U* test or by the Student's *t* test for unpaired data, using the InStat 3 program (GraphPAD Software for Science, San Diego, CA). Significant differences were accepted at  $P < 0.05$ .

## Results

### AEA modulates the temperature sensitivity of human PLTs

In a first series of experiments, we investigated the effects of the storage temperature on platelet viability. To this aim, human PLTs were incubated at either 22 or 37°C, and MTT assay was used to evaluate cell viability over time. PLTs were found to be temperature-sensitive, as they died faster when incubated at 37°C than at 22°C (Fig. 1). In fact,  $\sim$ 50% of MTT activity was lost after 24 h,  $\sim$ 80% after 48 h, and  $\sim$ 100% after 72 h of incubation at 37°C, whereas, at 22°C, PLT viability did not significantly change over the same period of time (Fig. 1).

In the presence of increasing concentrations of AEA (from 0.1 to 10  $\mu$ M), PLTs incubated at 37°C for 24 h showed increased survival. The most effective concentration of AEA was 1  $\mu$ M, that doubled the percentage of viable cells, while 10  $\mu$ M AEA was less protective (Fig. 2a). Thus, we chose to perform all subsequent experiments using AEA at 1  $\mu$ M concentration.

### AEA-mediated protection is triggered by CB<sub>1</sub>-dependent signaling

Next, we sought to gain further insight into the mechanism(s) of the AEA-mediated protective effects. PLTs can

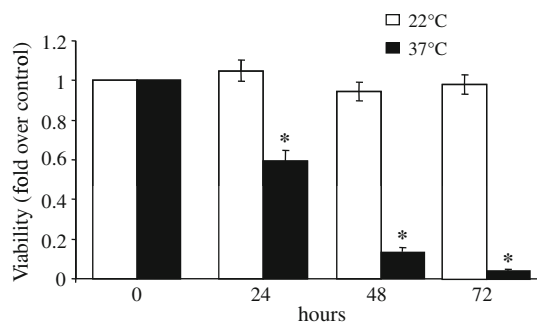


**Fig. 1** Temperature sensitivity of human platelets. Platelets were stored at either 22°C (white bars) or 37°C (black bars) for up to 72 h. At the indicated time points, cells were harvested and their viability was assessed by MTT. Values are reported as fold over control (arbitrarily set to 1). The data represent the mean  $\pm$  SD of at least four independent experiments, each performed in quintuplicate. \* $P < 0.01$  vs platelets incubated at 22°C

efficiently internalize and hydrolyze AEA through a membrane transport mechanism and FAAH [18]. However, intracellular uptake and breakdown of AEA did not appear to have a role in PLT viability. In fact, their survival when incubated with increasing concentrations (from 0.01 to 10  $\mu$ M) of Met-AEA, the non-hydrolyzable analogue of AEA, was superimposable on that elicited by AEA. As reported for many physiological processes [28, 29], the dose–response curve was bell-shaped, with a peak at 0.1  $\mu$ M Met-AEA (Fig. 2b). Met-AEA slightly increased PLT survival at 22°C (electronic supplementary material, ESM, Fig. 1A); at 37°C, the Met-AEA effects were evident for no longer than 48 h (ESM, Fig. 1B). Hydrolysis of AEA by FAAH generates AA [18]. Therefore, we checked whether the stimulatory effect of AEA on PLT viability could be mediated by AA potentially derived from AEA hydrolysis. We observed that the stimulatory effect of 1  $\mu$ M AEA was not reduced but rather enhanced by 100 nM URB597 (Fig. 2c), a selective inhibitor of FAAH. Additionally, AA up to 10  $\mu$ M exerted opposite effects compared to AEA, that is a dose-dependent induction of cell death (Fig. 2c). Altogether, these data rule out that the pro-survival activity of AEA on PLTs could depend on the by-product of AEA hydrolysis, AA. Moreover, to evaluate the possible site of action of AEA, we inhibited its cellular uptake by using 100 nM OMDM1, a selective inhibitor of AEA transport. This compound enhanced the protective effects of AEA (Fig. 3a), further suggesting an extracellular target for the action of this eCB.

Since AEA activates different signaling pathways depending on the receptor engaged, we investigated the effect of selective receptor antagonists. PLTs were pre-treated with either specific cannabinoid receptor antagonists (1  $\mu$ M SR141716 and 1  $\mu$ M SR144528, for CB<sub>1</sub> and CB<sub>2</sub> receptors, respectively), or with an antagonist of

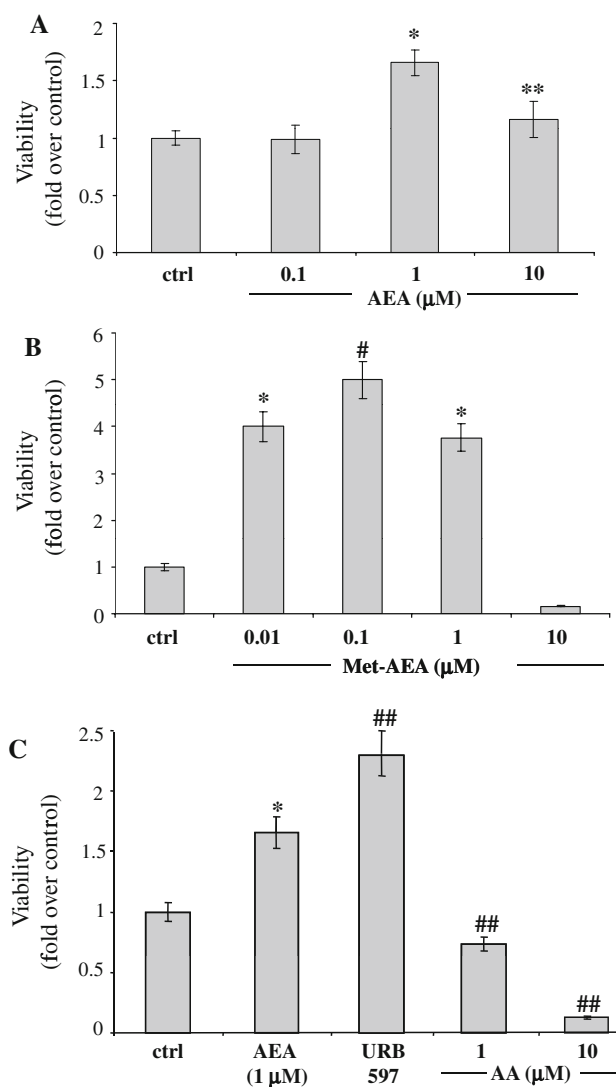


**Fig. 2** Effect of AEA on viability of human platelets. **a** Platelet viability in the presence of AEA. Cells were incubated at 37°C for 24 h, in the absence (*ctrl*) or in the presence of increasing concentrations (0.1–10  $\mu$ M) of AEA. **b** Platelet viability in the presence of the AEA non-hydrolyzable analogue Met-AEA. Cells were treated as reported in panel (a), using increasing concentrations (0.01–10  $\mu$ M) of Met-AEA. **c** Platelet viability in the presence of URB597 and AA. Cells were incubated at 37°C for 24 h, in the absence (*ctrl*) or in the presence of 1  $\mu$ M AEA, before or after 30 min pre-incubation with 0.1  $\mu$ M URB597 (a selective inhibitor of FAAH). Other samples were incubated with 1–10  $\mu$ M AA, a by-product of AEA hydrolysis. Values are reported as fold over control (arbitrarily set to 1). The data represent the mean  $\pm$  SD of at least five independent experiments, each performed in quintuplicate. # $P < 0.001$  vs control, \* $P < 0.01$  vs control, \*\* $P < 0.05$  vs control, ## $P < 0.01$  vs AEA-treated platelets

TRPV1 (1  $\mu$ M IRTX); then, PLTs were incubated at 37°C for 24 h in the presence of 1  $\mu$ M AEA or 0.1  $\mu$ M Met-AEA. As shown in Fig. 3a, 1  $\mu$ M SR141716 prevented the AEA- or Met-AEA-mediated survival of PLTs. Also, a different CB<sub>1</sub> antagonist like AM281 (used at 1  $\mu$ M) led to

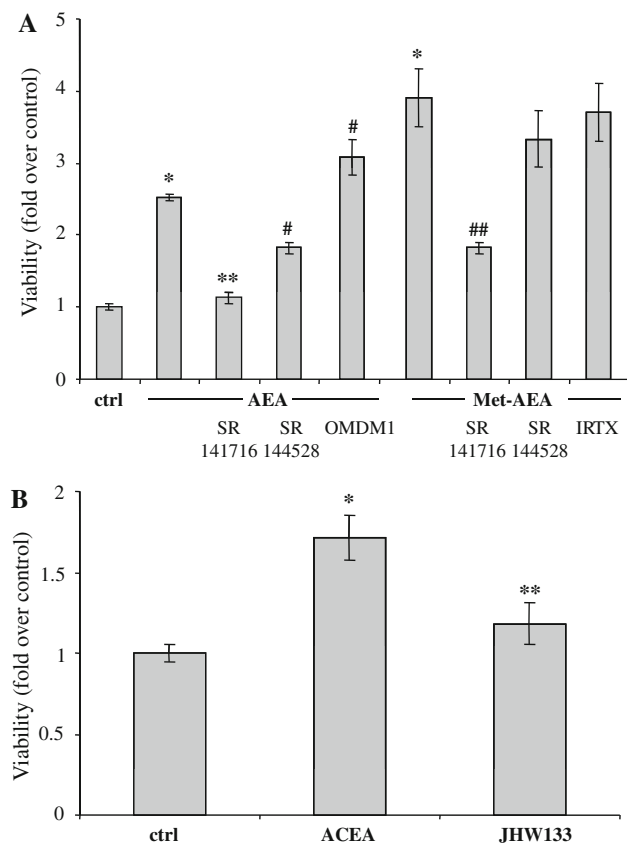


**Fig. 3** Effect of AEA and related compounds on viability of human platelets. **a** Platelet viability in the presence of AEA and related compounds. Cells were incubated at 37°C for 24 h, in the absence (*ctrl*) or in the presence of either 1  $\mu$ M AEA or 0.1  $\mu$ M Met-AEA, before or after 30 min pre-incubation with different compounds. Drugs used were: specific CB<sub>1</sub> (1  $\mu$ M SR141716, SR1), CB<sub>2</sub> (1  $\mu$ M SR144528, SR2) or TRPV1 (1  $\mu$ M IRTX) receptor antagonists, or a specific inhibitor of AEA transport (1  $\mu$ M OMDM1). \**P* < 0.01 vs control, \*\**P* < 0.01 vs AEA-treated platelets, #*P* < 0.05 vs AEA-treated platelets, ##*P* < 0.01 vs Met-AEA-treated platelets. **b** Platelet viability in the presence of CB<sub>1</sub> and CB<sub>2</sub> receptor agonists. Cells were incubated at 37°C for 24 h, in the absence (*ctrl*) or in the presence of either 1  $\mu$ M ACEA (CB<sub>1</sub> agonist) or 1  $\mu$ M JHW133 (CB<sub>2</sub> agonist). Values are reported as fold over control (arbitrarily set to 1); data represent the mean  $\pm$  SD of at least four independent experiments, each performed in quintuplicate. \**P* < 0.01 vs control, \*\**P* < 0.05 vs control

the same results observed with SR141716, further supporting the involvement of CB<sub>1</sub> (ESM, Fig. 2). Instead, SR144528 inhibited the effect of AEA or Met-AEA to a lower extent, and IRTX was not effective at all (Fig. 3a). Additional proofs for the involvement of cannabinoid receptors was obtained through the use of specific CB<sub>1</sub>, CB<sub>2</sub>, or TRPV1 agonists like ACEA, JHW133, or capsaicin, respectively. Treatment with 1  $\mu$ M ACEA increased by  $\sim$ 2-fold PLTs viability at 37°C compared to untreated cells, whereas 1  $\mu$ M JHW133 was much less effective (Fig. 3b), and 1  $\mu$ M capsaicin was not effective at all (not shown). Taken together, it can be concluded that CB<sub>1</sub>, and

to a lesser extent CB<sub>2</sub>, mediate the ability of AEA to prolong the life span of PLTs, whereas TRPV1 does not take part in this process. On this basis, we sought to further dissect the signaling pathways that led to PLTs survival through CB<sub>1</sub> activation. Since the effect of 1  $\mu$ M AEA was obtained by a 10-fold lower concentration (0.1  $\mu$ M) of its non-hydrolyzable analogue Met-AEA, we chose to carry out all the subsequent experiments with the latter compound at the concentration of 0.1  $\mu$ M.

#### CB<sub>1</sub> receptor signaling prevents cytochrome *c* release and caspase activation

In order to ascertain whether CB<sub>1</sub> receptor engagement could stimulate PLTs programmed cell death, some hallmarks of apoptosis were analyzed, such as cytochrome *c* release and caspase activation. First of all, we checked the subcellular localization of cytochrome *c* after temperature shifting. PLTs stressed by a higher temperature (37°C) showed a loss of mitochondrial cytochrome *c* and an increase in the cytosolic one. In agreement with the MTT data, 0.1  $\mu$ M Met-AEA was able to counteract this effect in a CB<sub>1</sub> receptor-dependent manner; indeed, the specific CB<sub>1</sub> antagonist SR141716 minimized the activity of Met-AEA (Fig. 4a).

Once released, cytochrome *c* is known to give rise to a ternary structure termed “apoptosome”, able to recruit and activate pro-caspase 9, which in turn activates effector caspases and triggers the cascade of events leading to apoptosis. Thus, we investigated the effect of Met-AEA on caspase activation. After 24 h of incubation at 37°C, larger amounts of the cleaved, active fragment (p35/37) of caspase 9 were found ( $\sim$ 2-fold) compared to PLTs stored at 22°C (Fig. 4b). Again, 0.1  $\mu$ M Met-AEA was able to counteract this effect, decreasing the amount of the cleaved product by  $\sim$ 2- to  $\sim$ 1.3-fold (Fig. 4b). Almost the same results were obtained when caspase 3 activity was checked: the enzymatic activity increased  $\sim$ 5-fold at a higher temperature, an effect that was halved by Met-AEA and restored in the presence of SR141716 (Fig. 4c).

Met-AEA does not work by modifying the Bcl-xL/Bak ratio

Mason et al. [24] elegantly demonstrated by phenotype-driven mutagenesis screen that the balance between anti-apoptotic Bcl-xL and pro-apoptotic Bak represents a biological clock for the platelet life span. Therefore, we checked whether Met-AEA was able to modulate this molecular timer.

As expected from induction of apoptosis, PLTs shifted from 22 to 37°C showed an altered expression of specific members of the Bcl-2 family. In particular, they showed an



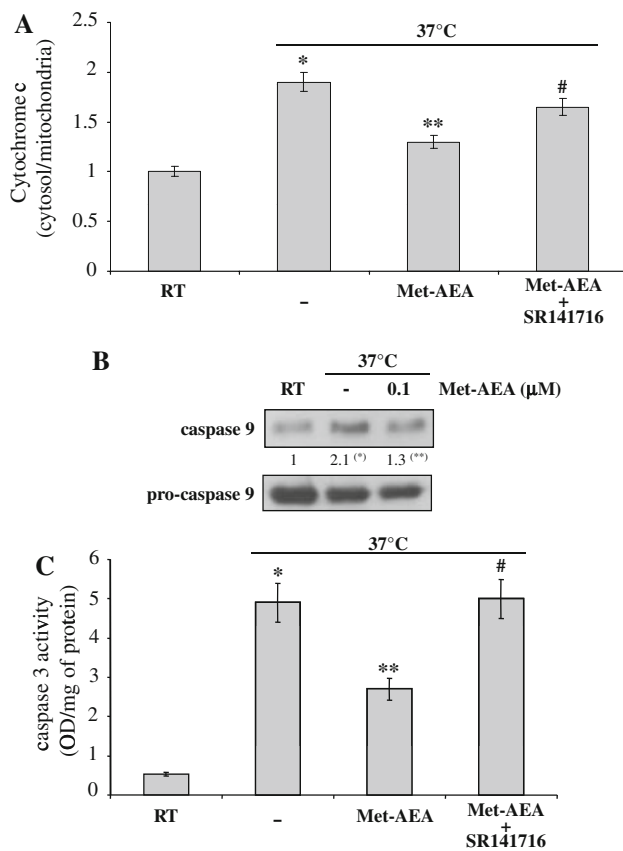


**Fig. 4** Effects of Met-AEA on apoptotic markers. **a** Cytochrome *c* release. Platelets were incubated either at 22°C (RT) or at 37°C (–) for 24 h; the indicated samples were also incubated in the presence of 0.1 μM Met-AEA, before or after 30 min pre-incubation with 1 μM SR141716 (CB<sub>1</sub> receptor antagonist). Cytochrome *c* release was evaluated by ELISA, performed both on cytosolic and mitochondrial fractions. Values are reported as ratios of cytosol/mitochondria cytochrome *c* content; data represent the mean ± SD of three independent experiments, each performed in duplicate. \**P* < 0.01 vs platelets stored at RT, \*\**P* < 0.05 vs platelets stored at 37°C, #*P* < 0.05 vs Met-AEA-treated platelets. **b** Western blot analysis of caspase 9. Platelets were incubated at 37°C, in the absence (–) or in the presence of 0.1 μM Met-AEA for 24 h; controls were platelets stored at 22°C (RT). Cell lysates were subjected to western blot analysis with the indicated antibodies, and expression levels were evaluated by densitometric analysis, reported above each band as numerical data. Values are the mean of three independent experiments (SD = 5%) and are reported as fold over control (arbitrarily set to 1), after normalization to the uncleaved form of caspase 9 (\**P* < 0.01 vs PLTs at 22°C, \*\**P* < 0.01 vs PLTs at 37°C). **c** Caspase 3 activity. Platelets were treated as reported in panel (b), then caspase 3 activity was measured. Values are reported as optical density (OD) values per milligram of protein; data represent the mean ± SD of three independent experiments, each performed in duplicate. \**P* < 0.01 vs platelets stored at RT, \*\**P* < 0.01 vs platelets stored at 37°C, #*P* < 0.01 vs Met-AEA-treated platelets

increased expression of Bak, while that of Bcl-xL was reduced (Fig. 5). Met-AEA was not able to modulate Bak and Bcl-xL levels, and blockade of the CB<sub>1</sub>/Met-AEA binding by SR141716 was ineffective (Fig. 5). Therefore, it can be suggested that the protective mechanism of action

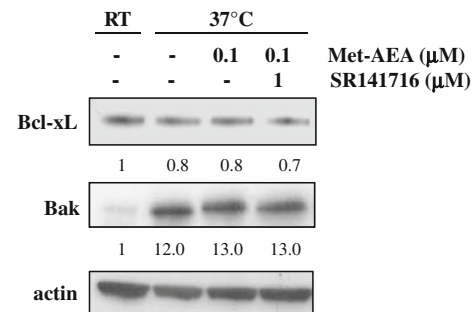


**Fig. 5** Effects of Met-AEA on Bcl-xL/Bak ratio. Analysis of Bcl-xL and Bak expression. Platelets were treated as detailed in Fig. 4b, then they were subjected to western blot analysis. Expression levels were evaluated by densitometric analysis, after normalization to actin. Numerical data below the bands are the mean of three independent experiments (SD = 7%) and are reported as fold over control (arbitrarily set to 1) (for all Bcl-xL bands *P* < 0.05 vs PLTs at 22°C, for all Bak bands *P* < 0.01 vs PLTs at 22°C)

of Met-AEA does not occur through an unbalance of the Bcl-xL/Bak ratio.

#### Met-AEA activates PI3K/Akt signaling

The anti-apoptotic role of PI3K/Akt signaling is well-documented in several cell types [30]. Here, we looked for the possible activation of Akt kinase by Met-AEA through phosphorylation of Ser 473 [30]. We found that cell death induced by incubation of PLTs at 37°C was paralleled by a remarkable decrease of Akt phosphorylation that returned to the levels observed in PLTs incubated at 22°C upon treatment with 0.1 μM Met-AEA (Figs 6a, b). Interestingly, at the same concentration, Met-AEA affected platelet survival (Fig. 2), indicating a relationship between these two phenomena (Fig. 6a). Moreover, an increased phosphorylation of Akt was an early, but sustained, event along the signaling pathway triggered by 0.1 μM Met-AEA, being already evident after 1 min of incubation (Fig. 6b). Then, it reached a peak at 5 min and afterwards it began to decline, although remaining higher than that observed in untreated PLTs incubated at 37°C (Fig. 6b). Accordingly, wortmannin, an inhibitor of PI3K, completely abolished the Met-AEA-mediated survival of PLTs, further supporting the involvement of the PI3K/Akt pathway in this process (Fig. 6c).

#### Activation of PI3K/Akt signaling regulates functional interactions among different members of Bcl-2 family

A mechanism by which Akt activity is coupled to protection against cell death is through the regulation of the pro-apoptotic protein Bad. Akt phosphorylates Bad at two serine residues, thus allowing its binding to 14-3-3 protein and sequestration into the cytoplasm. In this way, Bad

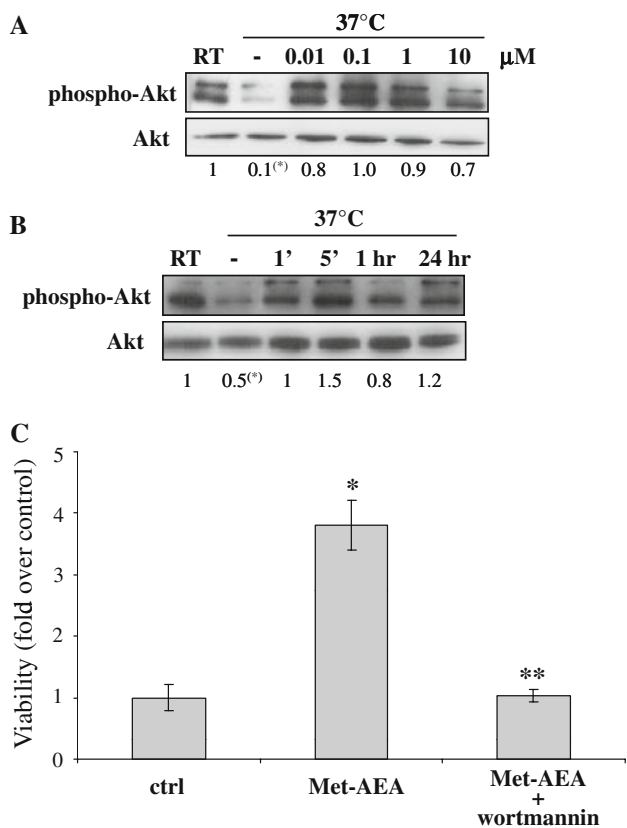


**Fig. 6** Effects of Met-AEA on Akt activation. **a** Dose–response curve of Akt phosphorylation. Platelets were incubated either at 22°C (RT) or at 37°C (–) for 5 min; the indicated samples were also incubated with increasing concentrations (0.01–10 μM) of Met-AEA. Phosphorylated Akt was detected by immunoblotting with anti-phospho-Akt antibodies (*upper panel*). In the *lower panel*, the amount of Akt is shown on the same filter, after re-probing with antibodies against Akt. Expression levels were evaluated by densitometric analysis (see *numerical data below the bands*); values are the mean of three independent experiments (SD = 5%) and are reported as fold over control (arbitrarily set to 1), after normalization to the levels of Akt (\* $P < 0.01$  vs PLTs at 22°C, all other samples  $P < 0.01$  vs PLTs at 37°C). **b** Time-dependent curve of Akt phosphorylation. Platelets were incubated at 37°C, in the absence (–) or in the presence of 0.1 μM Met-AEA, for the indicated periods of time; controls were platelets incubated at 22°C (RT). Phosphorylated Akt (*upper panel*) and Akt (*lower panel*) were detected as reported in panel (a). Expression levels were evaluated by densitometric analysis (see *numerical data below the bands*); values are the mean of three independent experiments (SD = 5%) and are reported as fold over control (arbitrarily set to 1), after normalization to the levels of Akt (\* $P < 0.01$  vs PLTs at 22°C, all other samples  $P < 0.01$  vs PLTs at 37°C). **c** Platelet viability in the presence of wortmannin. Cells were incubated at 37°C for 24 h, in the absence (*ctrl*) or in the presence of 0.1 μM Met-AEA, with or without 30 min pre-incubation with 100 nM wortmannin (the highest wortmannin concentration not presenting any effect on viability was chosen through dose–response experiments; see ESM, Fig. 3). \* $P < 0.01$  vs control, \*\* $P < 0.01$  vs Met-AEA-treated platelets

cannot enter the mitochondrion and make a heterodimer with the survival protein Bcl-xL (or Bcl-2), hence starting a death-promoting activity [30, 31]. To check whether Akt

activation following CB<sub>1</sub> receptor stimulation was indeed affecting Bad, we analyzed phospho-Bad levels in temperature-stressed PLTs, in the presence or in the absence of Met-AEA. PLTs undergoing cell death showed an increased protein level of Bad, most of which was in the dephosphorylated form (Fig. 7a, lane 2). Conversely, the presence of 0.1 μM Met-AEA promoted Bad phosphorylation, which increased ~6-fold compared to PLTs incubated alone at 37°C (Fig. 7a, lane 3). This effect of Met-AEA was clearly dependent on CB<sub>1</sub> receptor, since pre-incubation with SR141716 completely prevented it (Fig. 7a, lane 4).

We next checked whether Bad phosphorylation was accompanied by a change of Bcl-xL interaction with death-promoting members of the Bcl-2 family (Bak and Bax), and/or in Bak/Bax oligomerization. Temperature shift resulted in a down-regulation of Bcl-xL expression irrespective of the presence of Met-AEA, as shown by immunoprecipitation experiments (Fig. 7b, upper panel). Nonetheless, when Met-AEA was present, higher amounts of Bak protein could be co-precipitated with Bcl-xL (Fig. 7b, lower panel). Thus, it is conceivable that CB<sub>1</sub> receptor stimulation led to Akt activation, which in turn promoted the sequestration of Bad into the cytosol. As a consequence, Bcl-xL freely interacted with Bak, thus avoiding the oligomerization of pro-apoptotic Bcl-2 family members. To test our hypothesis, we analyzed the effect of Met-AEA on Bak and Bax activation. As shown in Fig. 7c, Bak oligomerization followed the temperature shift from 22 to 37°C, but in the presence of 0.1 μM Met-AEA the amount of Bak dimers significantly decreased. This effect could be reverted by blocking Met-AEA/CB<sub>1</sub> receptor interaction with SR141716. A similar pattern was observed when Bax dimers were analyzed, in the absence or in the presence of either SR141716 (Fig. 7d) or AM281 (ESM, Fig. 4).

Taken together, these results strongly suggest that Met-AEA mediates platelet survival by modulating the interactions among different Bcl-2 family members, which are key regulators of the mitochondrial death pathway.

## Discussion

Apoptosis is the main physiologic mechanism regulating the life span of cells, and is able to selectively delete unwanted cells. Nevertheless, this type of death has been restricted for a long time exclusively to nucleated cells, where it causes morphological and biochemical changes that allow removal by phagocytes without undesired inflammatory responses. Recently, it has been suggested that nucleus itself is not strictly required for apoptosis, as anucleated cells like erythrocytes and PLTs can also

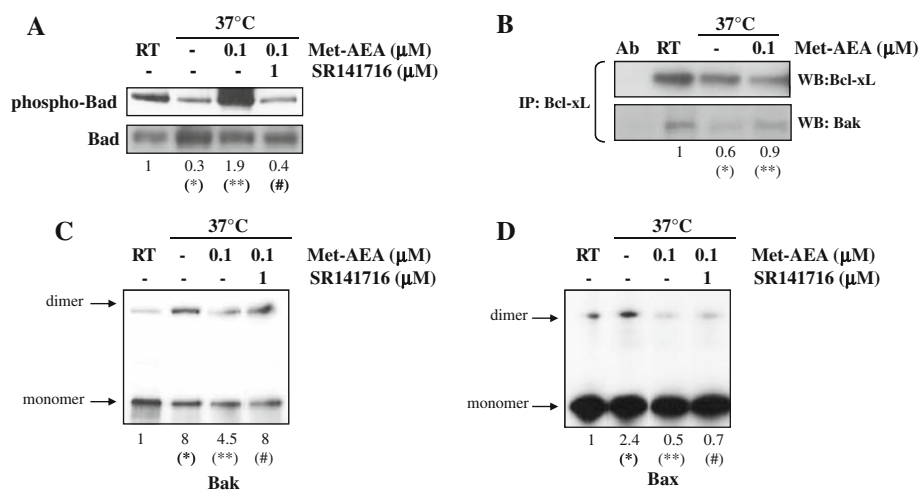


**Fig. 7** Effects of Met-AEA on Bcl-2 family members. **a** Analysis of Bad phosphorylation levels. Platelets were incubated at 37°C for 24 h, in the absence (–) or in the presence of 0.1 μM Met-AEA, as such or after 30 min pre-incubation with 1 μM SR141716; controls were platelets incubated at 22°C (RT). Phosphorylated Bad was detected by immunoblotting with anti-phospho-Bad antibodies (*upper panel*). In the *lower panel*, the amount of Bad is shown on the same filter after re-probing with antibodies against Bad. Expression levels were evaluated by densitometric analysis (see *numerical data below the bands*); values are the mean of three independent experiments (SD = 6%) and are reported as fold over control (arbitrarily set to 1), after normalization to the levels of Bad (\**P* < 0.01 vs PLTs at 22°C, \*\**P* < 0.01 vs PLTs at 37°C, #*P* < 0.01 vs PLTs treated with Met-AEA). **b** Analysis of Bcl-xL/Bak interactions. Platelets were treated as reported in panel (a), and were harvested after 24 h. Bcl-xL was immunoprecipitated from cell lysates and the immunoprecipitates were assessed by western blot analysis for Bcl-xL (*upper panel*) or Bak (*lower panel*). Ab represents the negative control (i.e., whole cell lysate immunoprecipitated in the absence of antibody). *Numerical data below the bands* represent the amount of co-precipitated proteins

compared to controls, arbitrarily set to 1. Values are the mean of three independent experiments (SD = 5%; \**P* < 0.01 vs PLTs at 22°C, \*\**P* < 0.01 vs PLTs at 37°C). **c** Analysis of Bak oligomerization. Platelets were treated as reported in panel (a) and, after 24 h, were subjected to western blot analysis. Oligomerization of Bak was monitored as the increase of higher molecular weight species corresponding to Bak dimers, and as the decrease of Bak monomers. *Numerical data below the bands* represent dimer/monomer Bak ratio compared to controls, arbitrarily set to 1. Values are the mean of three independent experiments (SD = 8%; \**P* < 0.01 vs PLTs at 22°C, \*\**P* < 0.01 vs PLTs at 37°C, #*P* < 0.01 vs PLTs treated with Met-AEA). **d** Analysis of Bax oligomerization. Platelets were treated as reported in panel (a) and, after 24 h, were subjected to western blot analysis. Oligomerization of Bax was monitored as the increase of higher molecular weight species corresponding to Bax dimers, and as the decrease of Bax monomers. *Numerical data below the bands* represent dimer/monomer Bax ratio compared to controls, arbitrarily set to 1. Values are the mean of three independent experiments (SD = 5%; \**P* < 0.01 vs PLTs at 22°C, \*\**P* < 0.01 vs PLTs at 37°C, #*P* < 0.01 vs PLTs treated with Met-AEA)

undergo programmed death. Just as an example, physiological platelet agonists (like thrombin and collagen), as well as platelet storage at 37°C, can cause apoptosis of these cells [23, 32], a phenomenon that can likely cause the thrombocytopenia observed in laboratory animals [24].

It has been speculated that eCBs and plant-derived cannabinoids regulate survival and death in a cell type-specific manner, that also depends on the receptors engaged [7, 8]. For instance, eCBs protect normal neurons and glial cells from apoptosis induced by exogenous factors (e.g., glutamatergic overstimulation, ischemia, and oxidative damage), whereas they significantly increase programmed cell death of tumor cells [15].

The present study shows a novel effect of the endocannabinoid AEA, that is, to extend the platelet life span by modulating the Akt-dependent phosphorylation of the proapoptotic factor Bad, thus modulating the interactions among different members of the Bcl-2 family. In agreement with previous reports [23, 33], we found that resting

PLTs, incubated at 37°C for up to 24 h, showed an enhanced expression of apoptotic proteins, including Bax, Bak, and caspases, while the expression of Bcl-xL appeared to be down-regulated. AEA promoted platelet survival through phosphorylation of Akt, which in turn phosphorylated Bad at Ser<sup>134</sup>, in this way preventing its binding to Bcl-xL and hence its pro-apoptotic activity. The protective effect of AEA appeared to be largely dependent on the signaling triggered by CB<sub>1</sub> receptor, as demonstrated by the effect of specific agonists and antagonists. These interactions are schematically represented in Fig. 8.

Previous studies have been focused on the ability of eCBs to modulate activation and aggregation of PLTs [16–19]. Much work has been done on this issue and, presently, it is well established that the two major eCBs (AEA and 2-arachidonoylglycerol) may activate platelets, alone or in synergy with other classical agonists [16–19]. However, it should be recalled that the effects of AEA or 2-arachidonoylglycerol on PLTs activation were observed



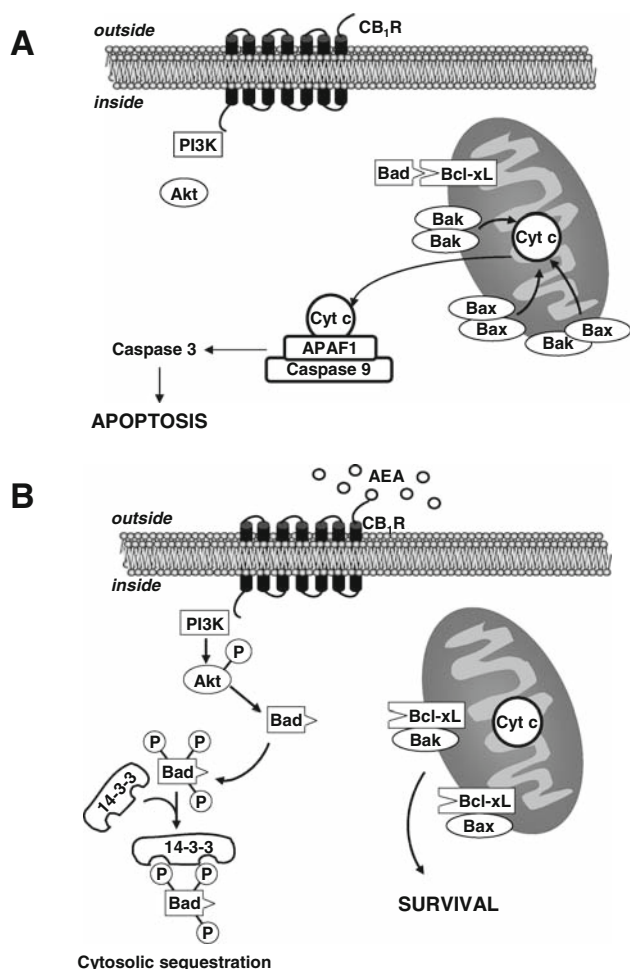


**Fig. 8** Possible regulation of survival/death of human platelets by AEA. **a** Platelets stored at 37°C activate the mitochondrial apoptotic machinery: *Bad* promotes cell death by displacing *Bak* (and *Bax*) from binding to *Bcl-xL*. Therefore, *Bak* and *Bax* are free to form oligomer channels in the mitochondrial membrane and to trigger cytochrome *c* release, that in turn activates the caspase 9 pathway leading to apoptosis. **b** Binding of AEA to *CB<sub>1</sub>R* receptor inhibits apoptosis by activating *PI3K/Akt* signaling: Akt-dependent phosphorylation of *Bad* promotes binding of *Bad* to 14-3-3 protein, thus preventing its association with *Bcl-xL*. As a consequence, *Bcl-xL* heterodimerizes with *Bak* and/or *Bax* proteins, thus antagonizing their apoptotic effect

at high micromolar concentrations that can be reached in PLTs [34], but are higher than blood levels [35, 36]. Indeed, AEA is present in blood plasma at nanomolar concentrations [35, 36]; nonetheless, its local concentration can be much higher, due to the local release of AEA by macrophages and endothelial cells [37, 38]. Thus, it is conceivable that the anti-apoptotic action of AEA observed may also occur in vivo. Incidentally, an opposite pro-apoptotic effect of AEA has been recently reported by Bentzen et al. [9] in erythrocytes, an observation that could be explained by cell-specific differences [7, 8], as well as by different experimental conditions.

It seems noteworthy that ex vivo platelet storage is performed at 22°C, in order to avoid a faster loss of viability compared to that observed at 37°C. Yet, in our body, PLTs survive at 37°C for 8–10 days. The discrepancy between in vivo and ex vivo conditions has been explained in terms of deprivation of some viability factors or accumulation of apoptosis-triggering signals. Indeed, plasma-free PLTs lose their function and undergo programmed cell death [33]. Our present data suggest that AEA present in blood may be one of the factors required for platelet survival. Such a role could be further complicated by the fact that low micromolar concentrations of AEA also stimulate haematopoiesis [39], and that PLTs are an important site of eCBs metabolism.

On a final note, it should be recalled that upon aging PLTs show a decreased level of *Bcl-xL*, which speeds up cell death [24]. Our results show that AEA does not change the *Bcl-xL/Bak* ratio, yet it affects the ability of *Bcl-xL* to interact with different members of the *Bcl-2* family. In this context, Akt is known to prevent *Bcl-xL* degradation during megakaryopoiesis [40], and it might be of interest to extend this finding to mature PLTs. In fact, in the latter cells, Akt may influence *Bcl-xL* turnover, possibly under the control of eCBs, thus providing another check-point for platelet homeostasis. Overall, this study contributes to the hypothesis that eCBs might represent an exciting therapeutic target for the inhibition of platelet demise in thrombocytopenias associated with enhanced apoptosis.

**Acknowledgments** This investigation was partly supported by Ministero dell'Istruzione, dell'Università e della Ricerca (PRIN 2007) to L.A., by Agenzia Spaziale Italiana (DCMC project) to A.F.A., and by Fondazione TERCAS (grant 2009–2012) to M.M.

## References

- Bari M, Battista N, Fezza F, Gasperi V, Maccarrone M (2006) New insights into endocannabinoid degradation and its therapeutic potential. *Mini Rev Med Chem* 6:257–268
- Di Marzo V (2008) Targeting the endocannabinoid system: to enhance or reduce? *Nat. Rev. Drug Discov.* 7:438–455
- Battista N, Gasperi V, Fezza F, Maccarrone M (2005) The anandamide membrane transporter and the therapeutic implications of its inhibition. *Therapy* 2:141–150
- McKinney MK, Cravatt BF (2005) Structure and function of fatty acid amide hydrolase. *Annu Rev Biochem* 74:411–432
- Katona I, Freund TF (2008) Endocannabinoid signaling as a synaptic circuit breaker in neurological disease. *Nat Med* 14:923–930
- Shimizu T (2009) Lipid mediators in health and disease: enzymes and receptors as therapeutic targets for the regulation of immunity and inflammation. *Annu Rev Pharmacol Toxicol* 49:123–150
- Maccarrone M, Finazzi-Agrò A (2003) The endocannabinoid system, anandamide and the regulation of mammalian cell apoptosis. *Cell Death Differ* 10:946–955

8. Pushkarev VM, Kovzun OI, Tronko MD (2008) Antineoplastic and apoptotic effects of cannabinoids. *N*-acylethanolamines: protectors or killers? *Exp Oncol* 30:6–21
9. Bari M, Battista N, Fezza F, Finazzi-Agrò A, Maccarrone M (2005) Lipid rafts control signaling of type-1 cannabinoid receptors in neuronal cells. Implications for anandamide-induced apoptosis. *J Biol Chem* 280:12212–12220
10. Bentzen PJ, Lang F (2007) Effect of anandamide on erythrocyte survival. *Cell Physiol Biochem* 20:1033–1042
11. Siegmund SV, Qian T, de Minicis S, Harvey-White J, Kunos G, Vinod KY, Hungund B, Schwabe RF (2007) The endocannabinoid 2-arachidonoyl glycerol induces death of hepatic stellate cells via mitochondrial reactive oxygen species. *FASEB J* 21:2798–2806
12. Dobrosi N, Tóth BI, Nagy G, Dózsa A, Géczy T, Nagy L, Zouboulis CC, Paus R, Kovács L, Bíró T (2008) Endocannabinoids enhance lipid synthesis and apoptosis of human sebocytes via cannabinoid receptor-2-mediated signaling. *FASEB J* 22:3685–3695
13. Turco MY, Matsukawa K, Czernik M, Gasperi V, Battista N, Della Salda L, Scapolo PA, Loi P, Maccarrone M, Ptak G (2008) High levels of anandamide, an endogenous cannabinoid, block the growth of sheep preimplantation embryos by inducing apoptosis and reversible arrest of cell proliferation. *Hum Reprod* 23:2331–2338
14. Gómez del Pulgar T, Velasco G, Guzmán M (2000) The CB1 cannabinoid receptor is coupled to the activation of protein kinase B/Akt. *Biochem J* 347:369–373
15. Viscomi MT, Oddi S, Latini L, Pasquariello N, Florenzano F, Bernardi G, Molinari M, Maccarrone M (2009) Selective CB2 receptor agonism protects central neurons from remote axotomy-induced apoptosis through the PI3K/Akt pathway. *J Neurosci* 29:4564–4570
16. Baldassarri S, Bretoni A, Bagarotti A, Sarasso C, Zanfa M, Catani MV, Avigliano L, Maccarrone M, Torti M, Sinigaglia F (2008) The endocannabinoid 2-arachidonoylglycerol activates human platelets through non-CB1/CB2 receptors. *J Thromb Haemost* 6:1772–1779
17. Malorni W, Bari M, Straface E, Battista N, Matarrese P, Finazzi-Agrò A, Del Principe D, Maccarrone M (2004) Morphological evidence that 2-arachidonoylglycerol is a true agonist of human platelets. *Thromb Haemost* 92:1159–1161
18. Maccarrone M, Bari M, Menichelli A, Del Principe D, Finazzi-Agrò A (1999) Anandamide activates human platelets through a pathway independent of the arachidonate cascade. *FEBS Lett* 447:277–282
19. Maccarrone M, Bari M, Del Principe D, Finazzi-Agrò A (2003) Activation of human platelets by 2 arachidonoylglycerol is enhanced by serotonin. *Thromb Haemost* 89:340–347
20. Italiano JE, Hartwig JH (2007) Megakaryocyte development and platelet formation. In: Michelson AD (ed) *Platelets*. Elsevier, San Diego, pp 23–44
21. Battinelli EM, Hartwig JH, Italiano JE Jr (2007) Delivering new insight into the biology of megakaryopoiesis and thrombopoiesis. *Curr Opin Hematol* 14:419–426
22. Catani MV, Fezza F, Baldassarri S, Gasperi V, Bretoni A, Pasquariello N, Finazzi-Agrò A, Sinigaglia F, Avigliano L, Maccarrone M (2009) Expression of the endocannabinoid system in the bi-potential HEL cell line: commitment to the megakaryoblastic lineage by 2-arachidonoylglycerol. *J Mol Med* 87:65–74
23. Bertino AM, Qi XQ, Li J, Xia Y, Kuter DJ (2003) Apoptotic markers are increased in platelets stored at 37 degrees C. *Transfusion* 43:857–866
24. Mason KD, Carpinelli MR, Fletcher JI, Collinge JE, Hilton AA, Ellis S, Kelly PN, Ekert PG, Metcalf D, Roberts AW, Huang DC, Kile BT (2007) Programmed anuclear cell death delimits platelet life span. *Cell* 128:1173–1186
25. Minn AJ, Kettlun CS, Liang H, Kelekar A, Vander Heiden MG, Chang BS, Fesik SW, Fill M, Thompson CB (1999) Bcl-xL regulates apoptosis by heterodimerization-dependent and -independent mechanisms. *EMBO J* 18:632–643
26. Degenhardt K, Sundararajan R, Lindsten T, Thompson C, White E (2002) Bax and Bak independently promote cytochrome C release from mitochondria. *J Biol Chem* 277:14127–14134
27. Gasperi V, Fezza F, Pasquariello N, Bari M, Oddi S, Finazzi-Agrò A, Maccarrone M (2007) Endocannabinoids in adipocytes during differentiation and their role in glucose uptake. *Cell Mol Life Sci* 64:219–229
28. Szabadi E (1977) A model of two functionally antagonistic receptor populations activated by the same agonist. *J Theor Biol* 69:101–112
29. Brown F, Graham JD, Taha SA (1973) Fade and desensitisation in guinea-pig ileum and vas deferens. *Eur J Pharmacol* 22:64–74
30. Datta SR, Brunet A, Greenberg ME (1999) Cellular survival: a play in three Akts. *Genes Dev* 13:2905–2927
31. Datta SR, Dudek H, Tao X, Masters S, Fu H, Gotoh Y, Greenberg ME (1997) Akt phosphorylation of BAD couples survival signals to the cell-intrinsic death machinery. *Cell* 91:231–241
32. Tonon G, Luo X, Greco NJ, Chen W, Shi Y, Jamieson GA (2002) Weak platelet agonists and U46619 induce apoptosis-like events in platelets, in the absence of phosphatidylserine exposure. *Thromb Res* 107:345–350
33. Brown SB, Clarke MC, Magowan L, Sanderson H, Savill JJ (2000) Constitutive death of platelets leading to scavenger receptor-mediated phagocytosis. A caspase-independent cell clearance program. *Biol Chem* 275:5987–5996
34. Maccarrone M, Bari M, Menichelli A, Giuliani E, Del Principe D, Finazzi-Agrò A (2001) Human platelets bind and degrade 2-arachidonoylglycerol, which activates these cells through a cannabinoid receptor. *Eur J Biochem* 268:819–825
35. Centonze D, Battistini L, Maccarrone M (2008) The endocannabinoid system in peripheral lymphocytes as a mirror of neuroinflammatory diseases. *Curr Pharm Des* 14:2370–2382
36. Giuffrida A, Piomelli D (1998) Isotope dilution GC/MS determination of anandamide and other fatty acylethanolamides in rat blood plasma. *FEBS Lett* 422:373–376
37. Wagner JA, Varga K, Ellis EF, Rzigalinski BA, Martin BR, Kunos G (1997) Activation of peripheral CB1 cannabinoid receptors in haemorrhagic shock. *Nature* 390:518–521
38. Deutsch DG, Goligorsky MS, Schmid PC, Krebsbach RJ, Schmid HH, Das SK, Dey SK, Arreaza G, Thorup C, Stefano G, Moore LC (1997) Production and physiological actions of anandamide in the vasculature of the rat kidney. *J Clin Invest* 100:1538–1546
39. Valk P, Verbakel S, Vankan Y, Hol S, Mancham S, Ploemacher R, Mayen A, Löwenberg B, Delwel R (1997) Anandamide, a natural ligand for the peripheral cannabinoid receptor is a novel synergistic growth factor for hematopoietic cells. *Blood* 90:1448–1457
40. Kozuma Y, Kojima H, Yuki S, Suzuki H, Nagasawa T (2007) Continuous expression of Bcl-xL protein during megakaryopoiesis is post-translationally regulated by thrombopoietin-mediated Akt activation, which prevents the cleavage of Bcl-xL. *J Thromb Haemost* 5:1274–1282